can analyze the transformation of the beam by the medium. During the first half-period, the size of the beam is given by (103) of Kogelnik [10], and we have another expression for the radius of curvature of the wavefront. In our experiment, w_0 given by (99) of Kogelnik [10], is equal to 0.65 mm when p is maximum. An incoming beam, with a spot size larger than w_0, is contracted by the medium, and we have a negative value for the radius of curvature of the wavefront. During the second half-period, we have an expression with hyperbolic functions, and the eflect is always defocusing.

For the stationary wave with $q=2$, the equivalent optical system is represented (Fig. 5) by a thin diverging lens of convergence $(-2\epsilon c)$ situated between two converging lenses of convergence c. Input and output ray slopes are shown as x_1' and x_4', respectively. A half-wavelength of medium has a convergence [1]: $2c=3n_0Alk^2p_M/2\pi\gamma RT$. The factor ϵ, equal to or less than unity, is used to take into account an asymmetry between the compression and the rarefaction of the medium, and a nonlinear variation of the index of refraction with the pressure. The frequency of this mode is given by

$$f=\frac{c}{2\pi a}\left[\left(\frac{3.83}{a}\right)^2+\left(\frac{2\pi}{l}\right)^2\right]^{1/2}. \qquad (4)$$

For our dimensions, this is equal to 14.7 kHz. The ray matrix of the system is given by the product of the matrices corresponding to each lens defined by (30) of Kogelnik [10]. The convergence of the system is equal to $c_1=2c(1-\epsilon)+lc^2-l^2c^3/2$. During the second half-period, we have a converging lens of convergence $2\epsilon c$ situated between two diverging lenses of convergence $(-\epsilon c)$. The system has a converging effect: $c_2=2c(1-\epsilon)+lc^2+l^2c^3/2$, which is almost the value obtained during the first half-period.

The value of the deflection can be obtained by measuring the displacement of a slot in front of the beam. The intensity of the light going through the slot is represented by equally spaced pulses. When we move the slot toward the edge of the deflected beam, the spacing between two pulses decreases, and they coincide when the slot is situated at the center of the maximum deflected beam. For the mode (0, 1) with no longitudinal variation, we have measured an angle of 3.3 minutes between the converging and the diverging deflections, for an incoming beam situated at 3 mm from the center of the cavity. A deflection of 23.4 minutes was obtained for the mode (2, 0) with no longitudinal variation which has two diametral planes of zero pressure. Near half the radius of the cavity, the Bessel function of zero order has a linear variation. Then the medium is equivalent to a prism, and for the modes with no longitudinal variation, the deflection is larger than near the center of the cavity.

For the mode (0, 1) with two nodal planes along the axis, the deflection is very small, and for a position of the slot near the inflection point of the Gaussian beam, we have an almost linear variation of the intensity with the deflection. By measuring the displacement of the slot, which gives the same variation, we can measure the deflection. We obtain an

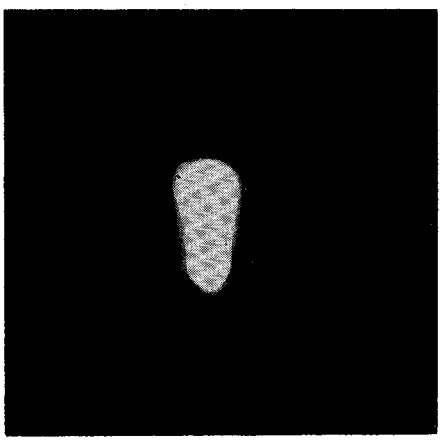

Fig. 6. Deflection due to the mode (0, 1) with no longitudinal variation.

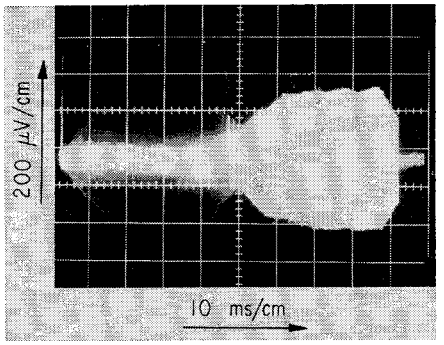

Fig. 7. Output of the phototube for the deflection of a beam near the center of the cavity, due to the mode (0, 1) with no longitudinal variation.

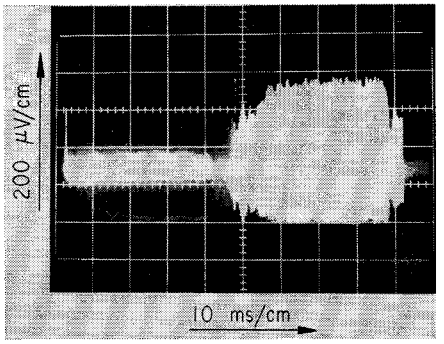

Fig. 8. Output of the phototube for the deflection of a beam near the center of the cavity, due to the mode (0, 1) with two nodal planes along the axis.

an angle of 2.9 seconds for an incoming beam situated at 3 mm from the center of the cavity. This value is 100 times larger than the calculated value with $\epsilon=1$ and corresponds to an asymmetry of 2.5 percent between the compression and the rarefaction. A measurement of the pressure along the axis and the diameter of the cavity would have been useful to determine whether the asymmetry actually exists or whether other perturbations explain the larger deflection than that expected.

Figure 6 shows the deflection obtained from the (0, 1) mode with no longitudinal variation of pressure. This figure represents the exposure of many cycles of the acoustic wave in sweeping the beam back and forth on the recording film. Figure 7 is a different representation of the deflection from this mode, with the phototube response shown on the oscillograph utilizing the slot method of detecting small deflections as described previously. Figure 8 shows a representation similar to that of Fig. 7 but for the mode (0, 1) with two nodal planes along the axis. Note the asymmetry of this picture which shows the net converging effect.

The work reported shows the possibility of obtaining appreciable deflection and focusing with acoustic gas lenses, and the differences between modes. The net focusing effect of the alternating-gradient system is observed. Additional measurements should be made with calibrated transducers in various places in order to compare experimental values with the calculated ones, and to determine the important asymmetries of the alternating-gradient system. Comparisons of liquid and gas acoustic lenses would also be desirable.

JACQUES KERDILES
J. R. WHINNERY
Electronics Research Lab.
and Dept. of Elec. Engrg.
University of California
Berkeley, Calif.

REFERENCES

[1] J. R. Whinnery, Bell Labs. unpublished memorandum, January 1964.
[2] P. K. Tien, J. P. Gordon, and J. R. Whinnery, "Focusing of a light beam of Gaussian field distribution in continuous and periodic lens-like media," *Proc. IEEE*, vol. 53, pp. 129–136, February 1965.
[3] W. H. Steier, "Some characteristics of alternating gradient optical transmission lines," *IEEE Trans. on Microwave Theory and Techniques*, vol. MTT-14, pp. 228–233, May 1966.
[4] J. R. Pierce, *Theory and Design of Electron Beams*. 2nd ed., Princeton, N. J.: Van Nostrand, 1954.
[5] A. J. DeMaria and G. E. Danielson, Jr., "Internal laser modulation by acoustic lens-like effects," *IEEE J. of Quantum Electronics*, vol. QE-2, pp. 157–164, July 1966.
[6] S. N. Rschevkin, *The Theory of Sound*. New York: Pergamon Press, 1963, p. 186.
[7] M. Redwood, *Mechanical Waveguides*. New York: Pergamon Press, 1960, ch. 3.
[8] H. Born and E. Wolf, *Principles of Optics*. New York: Pergamon Press, 1964, p. 87.
[9] D. Berlincourt and H. Jaffe, "Elastic and piezoelectric coefficients of single-crystal barium titanate," *Phys. Rev.*, vol. 111, pp. 143–148, July 1958.
[10] H. Kogelnik, "Imaging of optical modes—resonator with internal lenses," *Bell Sys. Tech. J.*, vol. 44, pp. 455–594, March 1965.

The Resonant Frequency of Interdigital Filter Elements

In a recent correspondence Nicholson [1] has described a method of predicting the center frequency of a bandpass interdigital filter. On the basis of existing techniques the design of this type of filter usually results in an error in the center and bandedge frequencies of the filter. The most important reason for this is the arbitrary manner in which the lengths of the fingers (i.e., center conductor) must be shortened at the open end [2]. By using

Manuscript received September 14, 1966; revised January 16, 1967.

Nicholson's method, it is possible to predict fairly accurately the distance between the end of the finger and the opposite end plate. The improved accuracy follows from the proper treatment given to the capacitances associated with the end of the finger. Gandhi and Khandelwal [3] and Khandelwal [4] have shown that these capacitances can also be included in the form of the effective length of a conductor (finger) in transverse TEM structures with an arbitrary conductor cross section. The interdigital structure is a special case of the transverse TEM structures.

The purpose of this correspondence is to indicate further refinements which may be added to the analysis of Nicholson. The equivalent length concept is used and techniques different from Nicholson's are employed for the calculation of the total end capacitance. In his analysis, the total end capacitance consists of the parallel plate capacitance between the finger tip and the opposite end plate, and the fringing capacitance between the finger tip and the side plates. However, no consideration has been given to:

1) The fringing capacitance between the finger tip and the end plate,
2) The interconductor capacitance when there is a given phase difference ϕ (equal to $\pi/2$ at the center frequency) between the adjacent conductors,
3) The effect of the end plate on the fringing capacitance, calculated as the discontinuity capacitance for the open-circuited line from Nicholson's Fig. 2; and
4) The fact that the interconductor capacitance is not contributed for a length x shown in Fig. 1.

While the first three effects increase the end capacitance and, hence, decrease the center frequency, the fourth tends to reduce the "effective length" and, hence, increases the center frequency of the filter.

In the case of geometrically simple finger cross sections, such as those that are rectangular or circular, all of the above factors can be accounted for without much difficulty. This is due to the possibility of equivalent zero thickness conductor representation [5] for simple geometries. For other cross sections, significantly more labor and additional approximations are involved. With regard to the interconductor capacitance it should be noted that most of it is contributed by the conductors in the immediate neighborhood of the conductor under consideration and therefore the effect of other conductors can be neglected.

For the effective length calculation, define C_0 and C_π, the zero- and π-phase capacitances [3], [4], as the total capacitance per unit length of a conductor with respect to ground when the phase difference between adjacent conductors is zero and π, respectively. Then the conductor capacitance per unit length to ground for any phase difference ϕ between the adjacent conductors is given as

$$C_\phi = C_0 + \tfrac{1}{2}(C_\pi - C_0)(1 - \cos\phi). \quad (1)$$

Thus for the filter at its center frequency where $\phi = \pi/2$,

$$C_{\pi/2} = \tfrac{1}{2}(C_\pi + C_0).$$

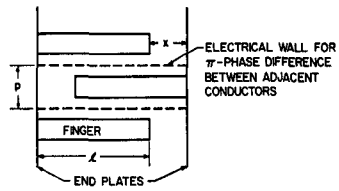

Fig. 1. Section of interdigital filter structure without top and bottom plates.

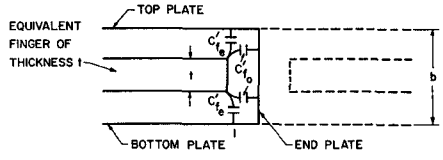

Fig. 2. Representation of a section of interdigital structure for the evaluation of the fringing capacitance associated with the conductor end.

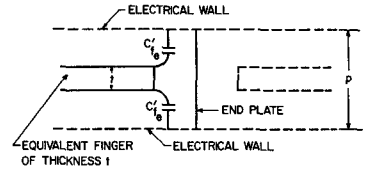

Fig. 3. Interdigital structure representation for evaluation of the fringing capacitance between adjacent conductors.

This capacitance gives the filter characteristic impedance as

$$Z_0 = \frac{\eta}{[(C_{\pi/2})/\epsilon_0\epsilon_r]},$$

where η is the characteristic impedance of free space. This impedance is usually chosen as 76 ohms for filter designs and optimum unloaded Q considerations. Thus for a total end capacitance C_t, the end capacitance equivalent length is $C_t/(C_{\pi/2})$.

To account for the situation at the shorted end a knowledge of the interconductor capacitance is required. This capacitance, which is zero for zero-phase difference between adjacent conductors and $4C_m$ per unit length for π-phase difference between adjacent conductors, will be $2C_m$ at the center frequency of the filter. C_m is the mutual capacitance between adjacent conductors when there is a π-phase difference between them. The equivalent negative length corresponding to this capacitance is

$$\frac{x \cdot 2C_m}{C_{\pi/2}}.$$

The "effective length" of the conductor can be written as

$$l_{eff} = l + \frac{C_t}{C_{\pi/2}} - \frac{x2C_m}{C_{\pi/2}}, \quad (2)$$

where l is the physical length of the conductor. The center frequency of the filter can be determined from the fact that the effective length should be equal to $\lambda/4$ at the center frequency.

To account for the fringing capacitance between the conductor end and the opposite end plate, Getsinger's [6] $2C_{f_0}'$ (Fig. 2) can be used rather than C_p alone. Here this capacitance will be denoted by C_e. Getsinger gives this capacitance for rectangular conductors which for the present case will be valid only when the conductor thickness is much smaller than its width. For the circular conductor case, Getsinger's results can be used by replacing the circular conductor by an equivalent zero-thickness conductor of a width equal to twice the diameter [5] (in the direction perpendicular to the plane of the paper). (In fact, a circular conductor can be represented by an equivalent rectangular conductor with one arbitrary dimension. The particular choice of zero thickness allows the edge effects to be neglected. It is for this reason that the use of equivalent zero-thickness conductors is recommended even for rectangular conductors.) The reasoning behind this calculation is apparent when a mirror image of the system about the end plate which is then treated as an electric wall is drawn (see Fig. 2).

The amount of fringing capacitance to the top and bottom plates can also be determined from the same geometry. This capacitance is equivalent to that given by Getsinger for rectangular conductors as C_{f_e}' and will be referred to here as C_{f_1}.

Again the zero- and π-phase capacitances approach will be used to account for the fringing capacitance between the adjacent conductors. For this case, the equivalent zero-thickness conductor will be placed perpendicular to the top and bottom plates (see Fig. 3). Clearly, the zero-phase capacitance in this case is zero and, hence, the $(\pi/2)$-phase capacitance C_{f_2} is just half of the π-phase capacitance which in turn can be calculated from a knowledge of Getsinger's C_{f_e}' by assuming an electric wall between the two adjacent conductors when they have a π-phase difference between them.

Two points are worth mentioning at this stage. First, the approximation of putting the electric wall midway between the adjacent conductors is not quite correct in the region between the finger end and the opposite wall, and will result in a slightly higher capacitance value. The exact location of the electric wall and, hence, the true capacitance can however be calculated from analog techniques. Second, one might question the use of C_{f_e}' for the calculation of these capacitances. However, this use is correct because a knowledge of the variation of Cristal's [7] mutual capacitance C_m between adjacent conductors when the spacing between the top and bottom ground planes is varied suggests the analogous behavior of the end plate capacitance in this case. The end plate thus reduces this fringing capacitance from Getsinger's C_f', which is 0.44ϵ for a zero-thickness conductor, to C_{f_e}' appropriate for this geometry. This leads to an important conclusion that in evaluating

the capacitance between two conductors, the effect of a third conductor is the same as that of a magnetic wall. However, there might be some additional capacitance between each conductor and the third one.

To demonstrate the use of the equivalent length concept, let us take the case of Cristal's [7] filter which was originally designed for a frequency of 1.5 GHz. Let us consider Cristal's resonators (fingers) 3 and 4 and their center-to-center spacing as pitch p. For the filter

$$C_0 = 4.5\epsilon_0$$
$$C_\pi = 5.372\epsilon_0$$
$$C_{\pi/2} = 4.93\epsilon_0 = 0.43684 \text{ pF/cm}$$
$$Z_0 = 76.38 \text{ ohms}$$

(width of equivalent zero thickness conductor) $w = 0.438$ inch. For C_e,

$$C_{f_0}' = 0.514\epsilon_0$$
$$C_e = 2wC_{f_0}' = 0.1012 \text{ pF}.$$

For C_{f_2},

$$C_{f_e}' = 0.3516\epsilon_0$$
$$C_{f_1} = 2wC_{f_e}' = 0.06927 \text{ pF}.$$

For C_{f_2},

$$C_{f_e}' = 0.350\epsilon_0$$
$$wC_{f_e}' = 0.03448 \text{ pF}$$
$$C_t = C_e + C_{f_1} + C_{f_2} = 0.20495 \text{ pF}.$$

The interconductor contribution to the π-phase capacitance for the structure is $4C_m = 4(0.210\epsilon_0)$. Thus the effective length of the conductor is

$$l_{eff} = 4.45 + \frac{0.20495}{0.43684} - \frac{(0.216)(2.54)(2C_m)}{0.43684}$$
$$= 4.87 \text{ cm}$$

and the corresponding center frequency of the filter is 1.54 GHz.

In conclusion, the present analysis gives a frequency slightly less than that predicted by Nicholson. However, better results will be obtained if the positions of the electric walls can be accurately evaluated, especially at the shorted end of the conductor. The effective length concept has been emphasized because it can be conveniently used in other applications of such structures. Furthermore, it can be easily improved upon by analog or rigorous analytic techniques based on conformal transformation methods.

D. D. KHANDELWAL
Electron Physics Lab.
University of Michigan
Ann Arbor, Mich.

REFERENCES

[1] B. F. Nicholson, "The resonant frequency of interdigital filter elements," *IEEE Trans. on Microwave Theory and Techniques (Correspondence)*, vol. MTT-14, pp. 250–251, May 1966.
[2] G. L. Matthaei, "Interdigital band-pass filters," *IRE Trans. on Microwave Theory and Techniques*, vol. MTT-10, pp. 479–491, November 1962.
[3] O. P. Gandhi and D. D. Khandelwal, "An improved version of the split-folded waveguide slow-wave structure," *Internat'l J. Electronics*, vol. 19, pp. 245–252, September 1965.
[4] D. D. Khandelwal, "Analysis of transverse TEM slow wave structures" (to be published).
[5] S. B. Cohn, "Problems in strip transmission lines," *IRE Trans. on Microwave Theory and Techniques*, vol. MTT-3, pp. 119–126, March 1955.
[6] W. J. Getsinger, "Coupled rectangular bars between parallel plates," *IRE Trans. on Microwave Theory and Techniques*, vol. MTT-10, pp. 65–72, January 1962.
[7] E. G. Cristal, "Coupled circular cylindrical rods between parallel ground planes," *IEEE Trans. on Microwave Theory and Techniques*, vol. MTT-12, pp. 428–439, July 1964.

Simplifying Maxwell's Equations in Gyrotropic Media

The purpose of this correspondence is to describe a method of handling Maxwell's equations in gyrotropic media. We have found this method to be particularly useful in the analysis of a small, ferrite filled waveguide, but believe it may be useful in general. The form of the equations appear to be considerably less complicated and capable of affording more insight than the methods employed in the literature [1]–[3]. We will make use of a pair of oppositely rotating, elliptically polarized vectors which, as is well known [4] can be used to diagonalize parts of the permeability, permittivity, and conductivity tensors. However, except in infinite media, these polarized variables will not simplify Maxwell's equations unless a new formulation is used.

For illustrative purposes, a gyromagnetic medium will be considered. The medium is taken to be magnetized in the z direction and a Cartesian coordinate system assumed. The time dependence and z variation are taken to be $e^{j\omega t}$ and $e^{-j\beta z}$, respectively. Only the magnetic equation of motion (permeability tensor) and Maxwell's two curl equations are required, as the divergence relations are redundant.

$$\nabla \times \boldsymbol{e} = -j\omega \boldsymbol{b} \qquad \nabla \times \boldsymbol{h} = j\omega \epsilon \boldsymbol{e}. \tag{3}$$

In matrix form

$$\begin{bmatrix} 0 & j\beta & \frac{\partial}{\partial y} \\ -j\beta & 0 & -\frac{\partial}{\partial x} \\ -\frac{\partial}{\partial y} & \frac{\partial}{\partial x} & 0 \end{bmatrix} \begin{bmatrix} e_x \\ e_y \\ e_z \end{bmatrix} = -j\omega \begin{bmatrix} b_x \\ b_y \\ b_z \end{bmatrix} \Bigg\| \begin{bmatrix} 0 & j\beta & \frac{\partial}{\partial y} \\ -j\beta & 0 & -\frac{\partial}{\partial x} \\ -\frac{\partial}{\partial y} & \frac{\partial}{\partial x} & 0 \end{bmatrix} \begin{bmatrix} h_x \\ h_y \\ h_z \end{bmatrix} = j\omega\epsilon \begin{bmatrix} e_x \\ e_y \\ e_z \end{bmatrix}. \tag{4}$$

DEFINITIONS

Let

$$b^{\pm} = b_x \pm jb_y.$$

Therefore,

$$b_x = \frac{b^+ + b^-}{2}; \qquad b_y = \frac{b^+ - b^-}{2j}.$$

Similar definitions are used for: $e^{\pm}$, $h^{\pm}$, e_x, e_y, h_x, h_y. We shall define two operators of the form

$$\nabla^{\pm} = \frac{\partial}{\partial x} \pm j\frac{\partial}{\partial y}.$$

Note

$$\nabla^+\nabla^- = \nabla^-\nabla^+ = \nabla_t^2$$
$$= \text{transverse divergence gradient.}^1$$

MAGNETIC EQUATIONS OF MOTION

The exchange-free, lossless, magnetic equation of motion can be manipulated to give the following set of equations [4]:

$$\begin{bmatrix} b_x \\ b_y \\ b_z \end{bmatrix} = \begin{bmatrix} \mu_{11} & j\mu_{12} & 0 \\ -j\mu_{12} & \mu_{11} & 0 \\ 0 & 0 & \mu_0 \end{bmatrix} \begin{bmatrix} h_x \\ h_y \\ h_z \end{bmatrix}. \tag{1}$$

Changing to polarized variables:

$$b^+ = \mu^+ h^+$$
$$b^- = \mu^- h^-$$
$$b_z = \mu_0 h_z \tag{2}$$

where:

$$\frac{\mu_{11}}{\mu_0} = 1 + \frac{\omega_m\omega_0}{\omega_0^2 - \omega^2}; \qquad \frac{\mu_{12}}{\mu_0} = \frac{\omega_m\omega}{\omega_0^2 - \omega^2}$$
$$\mu^+ = \mu_{11} + \mu_{12} = \mu_0\left(1 + \frac{\omega_m}{\omega_0 - \omega}\right)$$
$$\mu^- = \mu_{11} - \mu_{12} = \mu_0\left(1 + \frac{\omega_m}{\omega_0 + \omega}\right)$$
$$\omega_m = \gamma 4\pi M_s$$
$$\omega_0 = \gamma H_{DC}$$
γ = gyromagnetic ratio
$4\pi M_s$ = saturation magnetization
H_{DC} = magnetic field present in gyrotropic medium
μ_0 = permeability of free space.

MAXWELL'S EQUATIONS

Due to the similarity of the curl equations, it is convenient to perform parallel operations as follows:

Manuscript received October 21, 1966.

[1] Similar results can be obtained for cylindrical coordinates in either of two ways. The first is by defining new variables like $b^{\pm} = b_r \pm jb_\phi$ and $\nabla^{\pm} = \partial/\partial r \pm j(1/r)\partial/\partial\phi$. With these definitions, the transverse divergence gradient, ∇_t^2 becomes $(1/r + \nabla^-)\nabla^+ = (1/r + \nabla^+)\nabla^-$. The second is by preserving the Cartesian definitions and simply transforming into cylindrical coordinates.